Multiple Čerenkov second-harmonic waves in a two-dimensional nonlinear photonic structure

Wenjie Wang,[1,2] Yan Sheng,[1,*] Yongfa Kong,[2] Ady Arie,[3] and Wieslaw Krolikowski[1]

[1]*Laser Physics Center, Research School of Physics and Engineering, Australian National University, ACT 0200, Australia*

[2]*School of Physics, Nankai University, Tianjin, 300071, China*

[3]*Department of Physical Electronics, School of Electrical Engineering, Tel-Aviv University, Tel Aviv 69978, Israel*

**Corresponding author: ysh111@physics.anu.edu.au*

Received August 6, 2010; revised October 2, 2010; accepted October 3, 2010;
posted October 13, 2010 (Doc. ID 133025); published November 8, 2010

We report simultaneous generation of multiple conical second-harmonic waves in a two-dimensional nonlinear photonic structure when illuminated by two overlapping noncollinear fundamental beams. We show that this phenomenon is caused by the nonlinear Čerenkov radiation emitted due to the interaction of photons from each constituent fundamental beam as well as the virtual one propagating along the bisector of the two beams. In addition, by studying the asymmetric geometry of the interaction, we uniquely verify the effects of reciprocal vectors on the Čerenkov-type second-harmonic generation in nonlinear photonic structures.

OCIS codes: 190.2620, 190.4410, 220.4000, 050.1940.

The second-harmonic generation (SHG) of a laser field has been intensively studied since the emergence of nonlinear optics. It is well established that the efficiency of the frequency doubling process depends crucially on the phase-matching relations between the interacting waves. In quadratic media, these conditions are often achieved by utilizing the quasi-phase-matching (QPM) technique [1] that involves a periodic modulation of the second-order nonlinearity [$\chi^{(2)}$] of the material. In ferroelectric crystals, such as $LiNbO_3$ or $LiTaO_3$, the QPM conditions can be easily realized by electric field poling [2]. The resulting one- or two-dimensional (2D) structures with spatially modulated quadratic nonlinearity are often called $\chi^{(2)}$ nonlinear photonic structures (NPSs) [3–5].

There is a common perception that efficient SHG in an NPS always requires fulfilment of the full vectorial phase-matching condition $2\mathbf{k}_1 - \mathbf{k}_2 = \mathbf{G}$, where $\mathbf{k}_1$, $\mathbf{k}_2$ represent wave vectors of the fundamental and second-harmonic (SH) waves and $\mathbf{G}$ is a reciprocal vector of $\chi^{(2)}$ modulation. However, it turns out that this is not always the case and strong SHG is also possible in a Čerenkov scheme with only the longitudinal phase-matching condition $|\mathbf{k}_2|\cos\theta = 2|\mathbf{k}_1|$ being satisfied, where θ is an angle between the fundamental and SH waves [6]. Furthermore, it has been shown recently that the emission intensity of such Čerenkov-type SHG is greatly enhanced by the presence of $\chi^{(2)}$ modulation in NPSs [7–9], even in the most extreme case of a single boundary between two oppositely oriented ferroelectric domains [10–12]. The exact physical origin of this enhancement is still unclear, and it is a subject of intense investigations considering either the role of the reciprocal vectors in the NPS [7] or enhancement of the quadratic nonlinearity on the domain walls [11,12].

In this Letter we study the Čerenkov SHG in a 2D periodic nonlinear photonic structure. In contrast to all previous studies that were performed with a single or two symmetric fundamental beams (FBs), we analyze emission of the SH in very general situation in the presence of two asymmetric FBs. This case describes, for instance, experimentally relevant application of photonic structures in realization of the pulse autocorrelators [13]. We find that, depending on the orientation of the FBs relative to the optical axis of the nonlinear crystal, the SH is emitted in a form of either one or three sets of rings. We show that this phenomenon is caused by the Čerenkov emission due to the interactions of photons from each constituent FB and a virtual one propagating along the bisector of the two fundamentals. In addition, by employing this asymmetric geometry of interaction, we demonstrate the effect of the reciprocal vectors on the enhancement of the Čerenkov SHG in NPS, taking advantage of the differences between the azimuthal intensity distribution of the SH waves.

We employ a 2D periodically poled stoichiometric lithium tantalate (SLT) crystal (thickness of 0.4 mm) with a rectangular lattice. The lengths of the two base vectors of the lattice are 8.5 and 9.4 μm, respectively. The ferroelectric domain pattern revealed by etching the surfaces of the sample is depicted in Fig. 1(a). The reversed domains are uniform over the whole sample despite

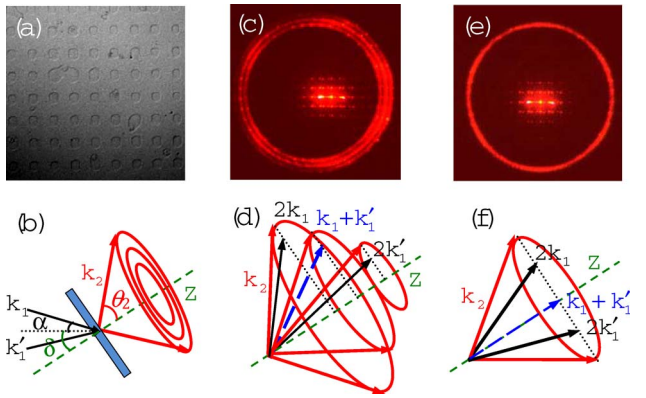

Fig. 1. (Color online) (a) Domain pattern of the 2D NPS. (b) Schematic of the experiment. (c), (e) Images of the SH rings observed with the asymmetric ($\delta \neq 0$) and symmetric ($\delta = 0$) FBs, respectively. (d), (f) Corresponding phase-matching diagrams.

0146-9592/10/223790-03$15.00/0

unavoidable variations on the domain shape and duty factor. After the imaging, both surfaces of the sample are polished for further experiments. As a light source, we use an optical parametric amplifier generating 150 fs pulses (250 Hz repitition rate, λ tunable from 1.2 to 1.6 μm). The laser beam is loosely focused by a cylindrical lens and then converted into two beams intersecting at an external angle of $2\alpha = 2 \times 5.18°$ by a bi-prism. The beam size of each pump waves at the input facet of the sample is about 100 μm $\times$ 2000 μm, which, for a given input power, corresponds to an intensity of about 10 GW/cm^2. The bisector of the two pumps is always directed along the horizontal direction of the laboratory coordinate system and forms an angle δ relative to the optical axis (Z axis) of the nonlinear crystal [see Fig. 1(b)]. The value of δ is adjustable by tuning the orientation of the crystal, which is placed on a rotation stage. A CCD camera is used to record the spatial intensity distribution of the SH waves on a screen located 29 mm behind the crystal and perpendicularly to the optical axis.

A typical image of the SH pattern with fundamental beams propagating asymmetrically with respect to the Z axis, i.e., $\delta \neq 0$, is shown in Fig. 1(c). Three rings with very close diameters are clearly seen. Two of them arise from the individual pump beams ($\mathbf{k}_1$ and $\mathbf{k}_1'$), and the third one (in the middle) appears only if the two fundamental beams cross inside the sample. All these rings have elliptical polarization at each azimuthal angle, because they are formed by ordinary and extraordinary conical beams overlapping due to the low birefringence of the crystal [7]. The differences between the propagation angles of these harmonic rings decrease when the FBs are closer to the directions symmetric with respect to the Z axis until they finally overlap into a single ring when $\delta = 0$ [Fig. 1(e)]. Inside the rings, close to the center, there is an additional SH structure. That one, which replicates the rectangular symmetry of the domain pattern, is formed as a result of the Raman–Nath nonlinear diffraction [14,15].

The SH emission in the form of multiple rings can be understood by considering the appropriate phase-matching conditions, which, for Čerenkov emission, depend only on the longitudinal direction. As shown in Fig. 1(d), each individual fundamental beam with the corresponding wave vector $\mathbf{k}_1$ (and $\mathbf{k}_1'$) induces an SHG with the conical angle θ_2 (and θ_2') defined as

$$|\mathbf{k}_2| \cos\theta_2 = 2|\mathbf{k}_1| \cos\theta_1, \tag{1}$$

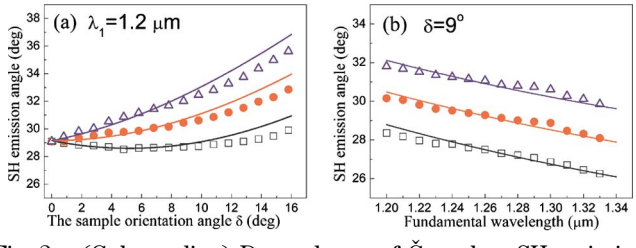

Fig. 2. (Color online) Dependence of Čerenkov SH emission angles as a function of (a) the sample orientation angle δ and (b) the wavelength of the FBs. The squares, triangles, and circles refer to the SH waves emitted by the individual FBs and the virtual beam, respectively. The solid curves are the theoretic predictions from Eqs. (1)–(3).

$$|\mathbf{k}_2| \cos\theta_2' = 2|\mathbf{k}_1| \cos\theta_1', \tag{2}$$

where θ_1 and θ_1' represent the incident angles of each fundamental beam inside the crystal and can be derived from the Snell's law: $n_1 \sin\theta_1 = \sin(\delta + \alpha)$ and $n_1 \sin\theta_1' = \sin(\delta - \alpha)$. The most interesting is the observation that the two beams can create a third Čerenkov ring in the middle. The two noncollinear beams act as an equivalent beam directed along their bisector, and this virtual (nonexistent) beam emits its own Čerenkov ring. The phase-matching condition of the Čerenkov harmonic emission from this virtual beam is written as

$$|\mathbf{k}_2| \cos\theta_2'' = |\mathbf{k}_1|(\cos\theta_1 + \cos\theta_1'). \tag{3}$$

While the nonlinear optical effects caused by the virtual beam have been discussed in the contexts of either Raman–Nath or perfectly phase-matched SHG [13,15], the Čerenkov-type SHG generated by virtual beam is demonstrated here for the first time, to the best of our knowledge.

Figure 2(a) depicts the measured values of the Čerenkov emission angles as a function of the sample orientation angle δ for the fundamental waves of $\lambda = 1.2$ μm. The results agree with the predictions of Eqs. (1)–(3) (using the refractive index published in [16]). When $\delta = 0$, only one Čerenkov angle is measured, because, at this extreme position, all three SH rings perfectly overlap. This agrees with the theoretical predictions that, given the condition of $\delta = 0$, Eqs. (1)–(3) lead to the same Čerenkov angle, i.e., $\theta_2 = \theta_2' = \theta_2''$. In Fig. 2(b), we display the variations of the Čerenkov angles with the wavelength (at fixed $\delta = 9°$). It is clear that the angles decrease gradually with the increase of the wavelengths. The measurements again agree well with the theoretic predictions. The emission angles measured in the experiment were smaller than the critical angle of SLT (≈28° inside the crystal), and therefore there was no risk of total internal reflection.

It is interesting that the Čerenkov SH rings exhibit quite asymmetric azimuthal intensity distributions. As shown in Fig. 1(c), the left side of the SH pattern is always weaker than the right one. To understand this phenomenon, we consider the effects of $\chi^{(2)}$ modulation. While the emission angle of the Čerenkov interaction is solely determined by the longitudinal phase-matching condition, the presence of $\chi^{(2)}$ modulation in the transverse direction can increase the rate of energy transfer from the fundamental to the SHs as the resulting reciprocal vectors may fully

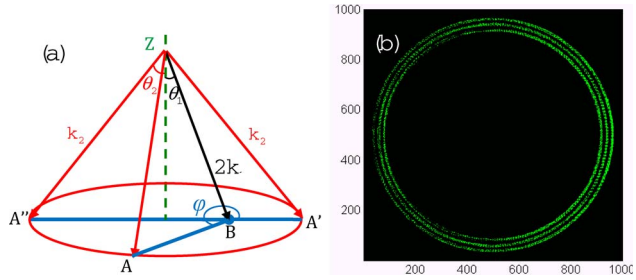

Fig. 3. (Color online) (a) Schematic of the phase-matching condition for a noncollinear fundamental beam. (b) Theoretically predicted intensity distribution of Čerenkov SHG obtained by $I_2 \propto \tilde{g}^2$.

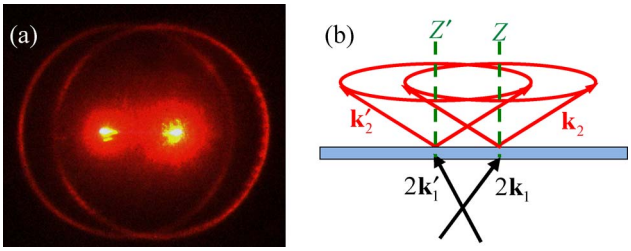

Fig. 4. (Color online) (a) SH pattern observed when the FBs cross outside the sample. (b) Corresponding interaction geometry.

compensate, or at least greatly reduce, the phase mismatch in the transverse direction. When the fundamental beams are incident along the directions asymmetric with respect to the Z axis of the crystal, as shown in Fig. 3(a), the magnitude of the reciprocal vector required by the transverse phase-matching condition is $AB = \sqrt{4|\mathbf{k}_1|^2 \sin^2\theta_1(\cos^2\varphi - 1) + |\mathbf{k}_2|^2 \sin^2\theta_2} - 2|\mathbf{k}_1| \sin\theta_1 \times \cos\varphi$, where φ is the azimuthal angle measured counterclockwise from the horizontal direction. It is clear that this magnitude takes different values at different azimuthal angles. The shortest one is $A'B = |\mathbf{k}_2| \sin\theta_2 - 2|\mathbf{k}_1| \sin\theta_1 \times (\varphi = 0)$, while the longest is $A''B = |\mathbf{k}_2| \sin\theta_2 + 2|\mathbf{k}_1| \times \sin\theta_1 (\varphi = \pi)$. For weak focusing of the pump and its negligible depletion, the QPM SH intensity is proportional to the square of the Fourier coefficient $\tilde{g}$ associated with the reciprocal vector $\mathbf{G}$. In Fig. 3(b), we plot the distribution of $\tilde{g}^2(\varphi)$ of those reciprocal vectors in our 2D structure, assuming a circular shape of reversed domains (radius $= 2.0$ μm) and taking $\delta = 5.75°$. It can be seen that the asymmetric intensity distribution of the Fourier spectrum closely reflects the actual experimental observations shown in Fig. 1(c).

Finally, we would like to stress that the simultaneous generation of the three Čerenkov rings occurs only if the two FBs cross inside the sample. When the sample is located far away from the bi-prism so the FBs do not overlap in the sample, only two Čerenkov rings originating from the individual pump beams are observed, as shown in Fig. 4(a). The centers of these two rings do not overlap anymore, which can be understood by the fact that, as shown in Fig. 4(b), in such case the beams interact with the sample at different spatial positions.

In conclusion, we have studied Čerenkov SHG in a 2D periodic nonlinear photonic structure with two intersecting fundamental beams. We have observed simultaneous generation of three Čerenkov rings that originate from the interactions of photons from each individual fundamental beam and a virtual beam propagating along the bisector of the two fundamental beams. We have discussed the azimuthal intensity distributions of these rings and have studied the variations of their propagation angles with the orientation of the fundamental beams, as well as with the wavelength. Applications of our results include nondestructive testing of domain structures, SH microscopy, and the monitoring of ultrashort pulses.

The authors acknowledge a financial support from the Australian Research Council and the Israel Science Foundation (ISF) (grant No. 774/09).

References

1. J. A. Amstrong, N. Bloembergen, J. Ducuing, and P. S. Pershan, Phys. Rev. **127**, 1918 (1962).
2. M. Houe and P. D. Townsend, J. Phys. D **28**, 1747 (1995).
3. V. Berger, Phys. Rev. Lett. **81**, 4136 (1998).
4. N. G. R. Broderick, G. W. Ross, H. L. Offerhaus, D. J. Richardson, and D. C. Hanna, Phys. Rev. Lett. **84**, 4345 (2000).
5. A. Arie and N. Voloch, Laser Photon. Rev. **4**, 355 (2010).
6. A. Zembrod, H. Puell, and J. Giordmaine, Opt. Quantum Electron. **1**, 64 (1969).
7. S. M. Saltiel, Y. Sheng, N. Bloch, D. N. Neshev, W. Krolikowski, A. Arie, K. Koynov, and Y. S. Kivshar, IEEE J. Quantum Electron. **45**, 1465 (2009).
8. Y. Sheng, S. M. Saltiel, W. Krolikowski, A. Arie, K. Koynov, and Y. S. Kivshar, Opt. Lett. **35**, 1317 (2010).
9. Y. Zhang, F. Wang, K. Geren, S. N. Zhu, and M. Xiao, Opt. Lett. **35**, 178 (2010).
10. Y. Sheng, A. Best, H. Butt, W. Krolikowski, A. Arie, and K. Koynov, Opt. Express **18**, 16539 (2010).
11. A. Fragemann, V. Pasiskevicus, and F. Laurell, Appl. Phys. Lett. **85**, 375 (2004).
12. X. Deng and X. Chen, Opt. Express **18**, 15597 (2010).
13. V. Roppo, D. Dumay, J. Trull, C. Cojocaru, S. M. Saltiel, K. Staliunas, R. Vilaseca, D. N. Neshev, W. Krolikowski, and Y. S. Kivshar, Opt. Express **16**, 14192 (2008).
14. S. M. Saltiel, D. N. Neshev, W. Krolikowski, R. Fisher, A. Arie, and Y. S. Kivshar, Phys. Rev. Lett. **100**, 103902 (2008).
15. S. M. Saltiel, D. N. Neshev, W. Krolikowski, N. Voloch-Bloch, A. Arie, O. Bang, and Y. S. Kivshar, Phys. Rev. Lett. **104**, 083902 (2010).
16. I. Dolev, A. Ganany-Padowicz, O. Gayer, A. Arie, J. Mangin, and G. Gadret, Appl. Phys. B **96**, 423 (2009).